

Anomalous Heat Production by Cavitation

Roger Stringham
First Gate Energies

2166 Old Middlefield Way, Mountain View, CA 94043, USA

ABSTRACT

The 40 KHz piezo reactor input exposes the $5 \times 5 \times 0.01 \text{ cm}^3$ foils to a controlled pulsed transient cavitation bubble, TCB, process with a peak acoustic input of one watt/cm². These TCBs are considered micro plasma accelerators. During its pseudo-adiabatic collapse a bubble jet is formed which accelerates a dense coherent plasma into a target foil. The pulse duration of the D⁺ injected into the foil lattice during an acoustic cycle is a few pico seconds. In the target foil anomalous heat, Q(x), is formed and produces as much as 15 watts over the 10 watt acoustic input. Calorimetric measurements of Q(x) use Newton's Law of Cooling where watts in equals watts out.

INTRODUCTION

Work began in April of 1989 as a chance opportunity to show that the anomalous heat produced by Pons and Fleischmann was worth investigation. I had experience using cavitation multi-bubble systems as an energy source [1]. This experience was converted into the M3C apparatus used in all recent experiments, an improvement on earlier systems [2]. The device, figure 2, is 6 kilos of machined Al that houses a 15 ml reactor through which D₂O is circulated. The reactor contains different metal foil targets which are exposed to cavitation under the same comparative conditions. The results of 75 runs of 24 hour duration at steadystate conditions (temperature, pressure, acoustic input, and D₂O flow rate) are examined. These runs are divided into several types: runs for calibration with the internal Joule heater, JH; runs that use foils that are active producers of Q(x); runs that are passive in the production of Q(x). The results of the calorimetric analysis of the data show that several elemental metal foils do produce Q(x) in excess of piezo and acoustic input, (A+B). The Q(x) correlates to the production of TCBs in the reactor. D₂O flows through the reactor at a regulated rate of 30 ml/min.. The reactor serves as a steadystate calorimeter measuring the watts input from the calibrated JH, encircling the outer reactor chamber. The calibration and sonication runs are made at steadystate conditions over a 24 hour period.

The calorimetric temperature measurements are obtained by multiple use of thermocouples, TC, that measure the temperature of the D₂O output from the reactor. The difference between an experimental

point on the JH calibration curve (on which any watt output, WO, point will fall) and the total output of acoustic plus anomalous heat, ((A+B)+Q(x)) = (WO), is a data point, see figure 2. Q(x) can be in terms of watts or delta temperature of the surface of the reactor.

Figure - 1

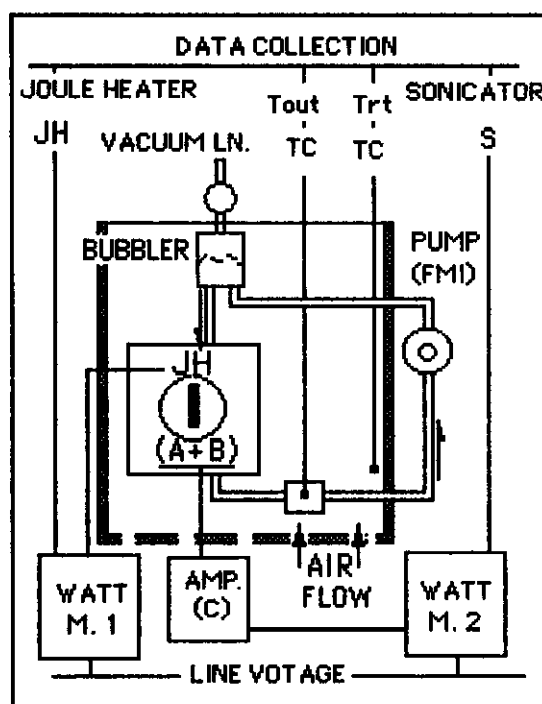


Figure 1. The schematic diagram of the calorimetric set up for the JH calibration and sonication runs. The M3C is the device used to gather reactor data. The runs are generally 24 hours allowing for long steadystate acquisition times for data collection. The apparatus is maintained at a constant flow of D₂O, at a constant temperature relative to rt, at a constant Ar pressure and at a constant acoustic input during its operation.

In these experiments the collapsing TCB is considered a micro accelerator injecting D⁺ into a target foil. The progression of the pseudo-adiabatic collapse, over a period of one μ sec., produces a bubble jet consisting of a dense coherent plasma in the order of $10^{20} \text{ D}^+ \text{ cm}^{-2} \text{ sec}^{-1}$ at the point of entrance

into the target foil. The pulse of D^+ injected into the foil lattice during an acoustic cycle is a few pico seconds; so in reality the D^+ flux density is several orders of magnitude higher [3]. The cause of $Q(x)$ is the collapse of the TCB on the target with the mechanism open to speculation.

EXPERIMENTAL

The containment consists of machined Al rings 14 cm in diameter that are bolted together to provide a vacuum tight reactor. Within and concentric with the containment is a reactor volume 60 mm diameter by 6 mm thick. The containment is fitted with 3 mm stainless steel tubing, a stainless steel and Pyrex bubbler and a displacement type circulation pump. See figure - 1.

The Al containment serves to hold two opposing acoustic piezo devices that are provided with circular stainless steel vibrating disks 6 mm apart. These disks also form the sides of the reactor and the bulk of exposed reactor surface area.

The orientation of the reactor containment, piezos and metal foil, is vertical. The two piezo devices provide an average of 2 to 10 watts of acoustic input to the D_2O in the M3C reactor with a line voltage efficiency, E . It varies from 0.33 to 0.43 ($E = S/(A+B)$) with, S , the sonicator input watts and $(A+B)$ the acoustic heating watts. S is measured by the M2 wattmeter and $(A+B)$ is measured by subtracting the calibrated amplifier watt heat loss, C , from S .

The piston type displacement pump from FMI, #QV1CSC, circulates D_2O at a constant rate of 30 ml/min. through the 15 ml reactor volume. The circulation path includes the pump, the reactor and the bubbler. The 30 ml. bubbler continuously removes bubbles and mixes the liquid and gases. The bubbler consists of stainless steel end plates capping a Pyrex cylinder, sealed with Teflon gaskets. The external pressure of Ar, P_x , is introduced and monitored at the bubbler. The reactor's variable JH is an ARI #BXX-04B-46-4K with a 120 ohm resistance with a 115 watt max. output which is measured by the M1 wattmeter.

CALORIMETRY

The system as a calorimeter (see Figure - 1) relies on its convection losses which are in balance with all heat input sources providing a continuous and steady input. These conditions produce the steadystate temperature, T_{ss} , in the device. A fan pushes a constant air flow past the apparatus surface producing a constant heat loss at the reactor surface at steadystate, T_{ss} . The heat loss is measured as WO for both the JH and $(A+B)$ input + $Q(x)$. The WO of the apparatus is established over a delta temperature ranging from 2 to 100°C delta ($T_{out}-T_{rt} = DT^{\circ}C$)

and is measured by 24 calibration runs interspersed between 51 foil runs. T_{out} is the temperature of the D_2O output and T_{rt} is the ambient temperature. The M3C requires three hours to reach 95% of the T_{ss} . The JH (or any heat or watt input) is represented by a best fit $DT^{\circ}C$ and WO equations;

$$DT^{\circ}C = 214(1 - e^{(-.003(WO + 3.3))}) \quad (1)$$

$$WO = (-1/.003(\ln(1 - DT^{\circ}C/214)) - 3.3). \quad (2)$$

The $(A+B) + Q(x) = WO$ at T_{ss} for 24 hours is the criteria for a measurement point, see figure 2.

Figure - 2

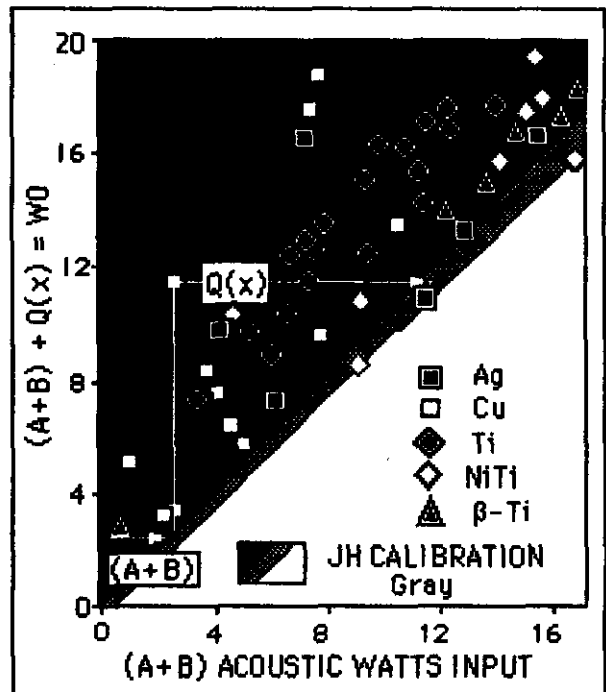


Figure 2. Above are the 51 steadystate 24 hour temperature runs for several metal foils. Any run (point) above the gray calibration curve produced $Q(x)$. $(A+B)$ is the acoustic watt input into the reactor and is calibrated with the reactor Joule heater. $Q(x)$ watts are the watts that must be added to bring watts in = to the watts out.

There are two opposing piezos, that makeup the 40 KHz acoustic input system which are pulsed 0.15 sec on and 0.85 sec. off. The resonating reactor containing the 15 ml of D_2O has a continuous acoustic wave input of about 90 watts maximum at 6 watts/ml of reactor volume making for an average pulsed input of 0.9 watts/ml for the 1.0 second duty cycle. The average output watts is determined from the calibration with JH. The $(A+B)$ is divided where (A) is the acoustic heating and (B) is the piezo

Figure - 3

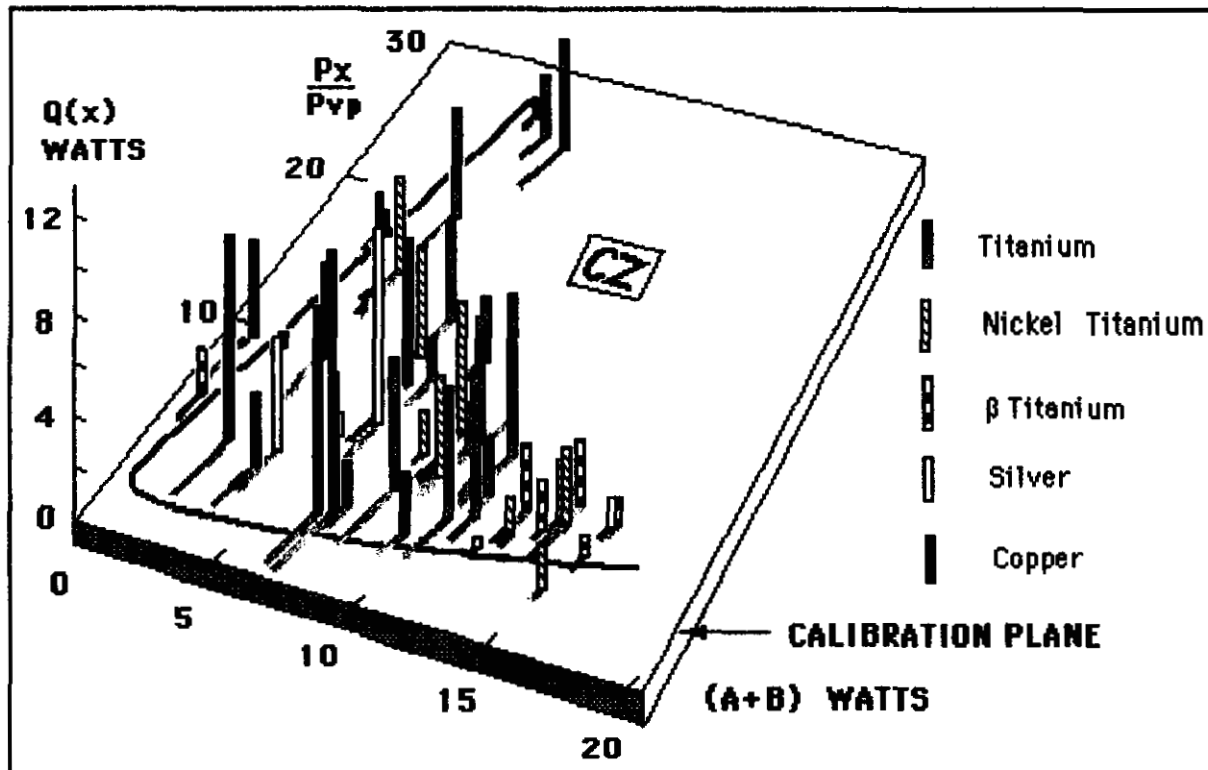


Figure 3. The 3 D portrayal of the anomalous heat, $Q(x)$, as projections from the (A+B), P_x/P_{vp} calibration plane. The controlling parameters P_x/P_{vp} and (A+B) determine the $Q(x)$ produced. The inside of the line on the calibration plane is the cavitation zone, CZ, and is favorable for $Q(x)$ production.

heating. The acoustic heating, (A), can be divided into two parts with (A₁) the pure acoustic heating of the liquid and (A₂) the cavitation heating of the liquid from the TCBs.

DATA

The apparatus was fitted with 8 thermocouples, pressure gauges, wattmeters and flowmeters with data taken at 5 minute intervals during the run. Data inputs were collected tracking the T_{out} , T_{rt} , T_{ss} , C, JH watts, and S watts driving the sonicator piezos. The analyses were focused mainly on the production of $Q(x)$. There has been in the past some examination of foils for unusual radiation activity, some foil surface examination by SEM showing ejecta sites [4.5] and some mass spectral analyses for He4, He3 and T [2]. The collection of steadystate results of the experiments over a period of two years are represented in figures 2 and 3.

To reveal relationships in the data scatter of $Q(x)$ a three dimensional treatment of 51 foil target runs interspersed with the 24 calibration runs is presented in figure 3. $Q(x)$ is shown as the distribution of projections, vertical black lines, from the P_x/P_{vp} ,

(A+B) plane. This gray plane is the calibration plane, where watts in = W₀. The vapor pressure, P_{vp} , of D2O is also a measure of its temperature. Keeping P_{vp} constant (constant temperature) and varying P_x and (A+B) shows that $Q(x)$ has a distribution similar to that of multi-bubble sonoluminescence, SL, intensity [6].

Figure 3 shows a curve on the calibration plane where the interior of the curve is the cavitation zone, CZ. Exterior to CZ, as (A+B) increases, there is D2O frothing and as P_x/P_{vp} increases there is bubble suppression. The influence of these two parameters on the TCB production is parallel to what is expected in SL bubble production.

The error in the measurement of $Q(x)$ is ± 1 watt. The error in the JH calibration measurements is ± 0.5 watts. The error measurement of JH, the gray of figure 2, is the same as for the JH calibration plane figure 3.

The production of TCBs require an environment that is a balance between P_x , P_{vp} , and (A+B). Large or small values for any of these controlling parameters lead to the absence of TCB formation and no $Q(x)$ production.

RESULTS

Evaluating the $Q(x)$ produced as it relates to that portion of $(A+B)$ that produces the TCBs, which is (A_2) , has not been done. Only a portion of (A) is used to produce TCBs in the D_2O , with the rest of the input going directly into heating the reactor. If $(A+B)$ is too small or the ratio of P_x/P_{vp} too large, no TCBs will form and this appears to be the case in figure 3 as very little $Q(x)$ is found outside of the line defining the CZ on the calibration plane.

In the calculations of $Q(x)$, $(A+B)$ was used and not the value for (A_2) . If the (A_2) could be determined, the relative ratio of $Q(x)/(A_2)$ would be 2 to 10 times larger than $Q(x)/(A+B)$ used. This makes the calculations for $Q(x)$ very conservative.

The pressure ratio, P_x/P_{vp} , is made up of two opposing parameters, P_x that tends to suppress and P_{vp} that tends to ease the TCB formation. The P_{vp} increases exponentially with a reactor temperature increase and must be kept in balance for TCB formation. The values for the pressure ratio, along with values for the $(A+B)$, indicate "a production mode" or "a non production mode" for $Q(x)$.

The three dimensional plot of $Q(x)$ is produced collectively by several different metal foils as shown in figure 3. The $Q(x)$ is reproducible and predictable if (A_2) , T_{ss} or P_{vp} , P_x and type of metal are known. At present the use of $(A+B)$ instead of (A_2) gives qualitative results when all the data is viewed together as a set. Individual foil types have different levels of $Q(x)$ production. The amount of $Q(x)$ production from foil types studied are listed in order starting with the best, Cu, then followed by Ag, Pd, NiTi, Ti and β Ti. The stainless steel foils, which is the major material of the reactor, show little if any $Q(x)$. Experiments have shown that a stainless steel foil in the reactor for comparative purposes produces zero $Q(x)$.

The CZ for (P_x/P_{vp}) ratio, a combination of temperature and external pressure, is the most effective at a value of around 50 ± 30 for the $Q(x)$ production.

It should be pointed out that metal foil types, their thickness, grain size and history all may influence the $Q(x)$ production. The fine grained metals are more durable and the thicker foils reflect much of the acoustic power. The reflection of the thicker foils implies much less acoustic energy density in the metal lattice and this is a factor in $Q(x)$ production.

The acoustic input to the reactor produces a standing wave resonance in the thin foil lattice that, after time, imprints the foil with a miniature image of the resonating bound foil. These foils are resonating in the MHz region and act as another acoustic source for bubble formation.

The foils exhibit, from their cavitation exposure, formation of ejecta sites originating in the lattice with

the condensation of 1μ metal spheres in and about the ejection sites. A calculation of the energy of one of these sites indicates that it is 10^6 times greater than a chemical reaction. The SEM analyses of these sites are evidence of rapid dissipation of small but very high temperature events occurring in the lattice [4]. Radiation analyses of the reactor and foils were negative for long range radiation emission. Some past mass spectral analyses show the formation of He4, He3 and T [2].

SUMMARY & FUTURE WORK

These experiments are easily performed. The treatment of the data shows that $Q(x)$ boundary conditions, CZ, as defined by the parameters P_x , P_{vp} , $(A+B)$ are similar to those for the production of TCBs and SL. For a given apparatus the steadystate relation must be found between $DT^\circ C$ and WO . The equations (1) and (2) accomplish this and $Q(x)$ is easily determined if $(A+B)$ is measured. In future work (A_2) will be measured for better results. It is felt that the TCBs jet formation and injection of D^+ into the foil is responsible for $Q(x)$.

There are other phenomena that connect with the production $Q(x)$ and these are helium production (analyses not performed in these experiments), ejecta sites that appear to be produced by unknown target lattice events, and possible transmutations [2].

A simplified acoustic technology will be incorporated into a static piezo reactor device, with no pump and no circulation of heavy water [3].

I would like to thank T. Passell, G. Kohn, R. Raymond, and Y. Takeuchi for their support.

REFERENCES

- [1] M. Toy, R. Stringham, "Photoassisted Sonosynthesis of 1,2,3,4 Tetrakis(mythylthio) hexafluorobutane," ACS Symposium, 278, 1985, p. 290.
- [2] R. Stringham, R George, "Cavitation-Induced Excess Heat in Deuterated Metals," EPRI Rept.TR-108474, Mar. 1998.
- [3] R. Stringham, J. Chandler, R. George, T. Passell, and D. Raymond, "Predictable and Reproducible Heat," ICCF-7 Conference Vancouver, BC, April 1998, p. 361.
- [4] R. George, Ejecta sites, *Scanning*, Apr 1997, p.
- [5] F. Okuyama, H. Tsujimaki, "Outflow of molten matter from deuterium-implanted sub-surface of palladium," *Surface Science*, 382, 1997, p. L700-L704.
- [6] R. Verrall, C. Segal, *Ultrasound*, ED. by K. Suslick, VCH, 1988, p. 269; A. Weissler, *J. Am. Acoust. Soc.*, 225, 1955, p. 651.